Energy Nexus 17 (2025) 100379

Contents lists available at ScienceDirect

Energy Nexus

journal homepage: www.elsevier.com/locate/nexus

Full Length Article

Techno-economic and life cycle greenhouse gas assessment of green ammonia produced by low-pressure Haber-Bosch process

Guohui Song [a,b,*], Yumeng Chen [a], Yingfeng He [a], Qize Jia [c,d], Qingjiao Wu [e], Xiaobo Cui [a,b,f], Hao Zhao [c,d,*]

[a] School of Energy and Power Engineering, Nanjing Institute of Technology, Nanjing, Jiangsu 211167, China
[b] Jiangsu Provincial Key Laboratory of Multi-energy Integration and Flexible Power Generation Technology, Nanjing Institute of Technology, Nanjing Jiangsu 211167, China
[c] College of Engineering, Peking University, Beijing 100871, China
[d] Institute of Energy, Peking University, Beijing 100871, China
[e] China Light Industry Wuhan Design & Engineering Co., Ltd., Wuhan 430060, China
[f] School of Energy and Environment, Southeast University, Nanjing 210096, China

ARTICLE INFO

Keywords:
Power-to-ammonia
Low-pressure
Energy efficiency
Greenhouse gas emission
Ammonia emission
Levelized cost of ammonia

ABSTRACT

Green ammonia can be used as an energy storage carrier and a sustainable chemical. To improve the competitiveness of green ammonia, two power-to-ammonia (PtA) processes integrated with low-pressure (LP) and ultra-low-pressure (ULP) Haber-Bosch (HB) techniques were designed and optimized based on technical, economic, and environmental performances. The effects of multiple variables were studied. The LP technique is preferred over the ULP technique because the latter has a more complex configuration and a slightly higher levelized cost. The systematic energy efficiency excluding or including the cold energy of liquid ammonia reaches 68.71 % or 73.75 %, respectively. The unit power consumption of green ammonia is as low as 7.64 kWh/kg. The plant scale should not be <10 t/h. Based on the electricity price for energy storage (0.041 €/kWh), the equivalent operating hours should exceed 5000 h to achieve profitability. The life cycle greenhouse gas emission of green ammonia derived from wind power under the Chinese scenario is 257–316 $kgCO_2e/t$. The life cycle ammonia emissions with NH_3 recovery from the purge gas is <0.06 $kgNH_3/t$. This study indicates that the PtA technology can efficiently store intermittent electricity with cold energy utilization and effectively decarbonize the ammonia industry.

1. Introduction

Ammonia is one of the most important chemicals due to its various uses. It can also be used as refrigerant and carbon-free fuel. Nowadays, green ammonia has great potential to play a substantial role as a hydrogen energy carrier. Ammonia has a gravimetric hydrogen content of 17.8 % and is one of the highest energy carriers [1]. It is easily liquefied by increasing pressure to ~10 bar at room temperature, or by cooling to −33 °C at atmospheric pressure. The volumetric energy density of liquid ammonia is 3 times higher than that of compressed hydrogen (69 MPa and 25 °C) [1], and 1.5~1.7 times higher than that of liquid H_2 (0.1 MPa, 20 K) [2]. Unlike liquid hydrogen, the technology of shipping and pipeline transfer of ammonia is well established in the existing industry. This infrastructure and existing regulations could be leveraged to guarantee reliable, ready, and safe ammonia distribution as a low-carbon energy vector [1]. At present, most ammonia is produced from fossil fuels. The global production of ammonia consumes 1–2 % of the global annual energy supply and accounts for approximately 1.5 % of all greenhouse gas emissions [3]. The sustainable production of ammonia is expected in the context of climate change.

Green power-to-ammonia (PtA) conversion is regarded as a sustainable pathway for green ammonia [3]. Recently, several important advances have been made, particularly in electrocatalysis [4,5] and plasma catalysis [6,7]. However, MacFarlane et al. predicted that the Haber-Bosch (HB) process-based ammonia synthesis solution would dominate the generation technology for at least the next decade [8]. It normally operates at high temperatures (400–500 °C) and pressures (10–30 MPa), commonly using an iron-based catalyst. The majority of

* Corresponding authors.
E-mail addresses: ghsong@njit.edu.cn (G. Song), h.zhao@pku.edu.cn (H. Zhao).

https://doi.org/10.1016/j.nexus.2025.100379
Received 28 September 2024; Received in revised form 25 November 2024; Accepted 8 February 2025
Available online 9 February 2025

assessment investigations on green ammonia production have been based on HB synthesis at a pressure of approximately 15 MPa [9,10,11].

The traditional HB process is energetically demanding, and decreasing the specific energy consumption is highly expected. Feasible measures are to develop an inexpensive yet efficient catalyst for ammonia synthesis under mild reaction conditions (<400 °C, <10 MPa) and to lower the operating pressure of the synthesis loop [12]. Several important advances have been made in the investigation of catalysts for ammonia synthesis under mild reaction conditions (0.1–7 MPa) [12–14]. The main challenge for practical application at such low pressures is the low reaction rate, according to previous studies on catalysts [12,13]. Another effect is to optimize the technical process. Ahmad Shamiri and Nia Aliabadi optimized an industrial ammonia synthesis reactor with a pressure of 8.6 MPa and improved indicators such as per-pass conversion and energy consumption [15]. Rouwenhorst conducted the technical and economic evaluation of power-to-ammonia-to-power for local electricity storage integrated with an ammonia synthesis reactor at 275 °C and 7.8 bar and adsorption separation at 150 °C [16], which is currently not a mature separation technology [17]. In comparison, the demonstration and application of low-pressure HB synthesis technologies (< 10 MPa) lag behind the trend in catalyst development.

Technology developers must consider the technical, economic, and potential environmental impacts while developing new sustainable technologies [18]. Previous assessments mainly focused on the techno-economic of ammonia produced by the HB process at high-pressure (≥15 MPa) [10,11,19]. The commercial ammonia derived from fossil feedstock has a carbon intensity of 1.5–4.19 tCO_2e/t [20,21]. It can be reduced to 0.77 $kgCO_2e/t$ with application of CO_2 capture [22]. To further abate carbon emissions, novel processes were explored, such as producing ammonia from food waste and brown water [23]. However, these technologies cannot play a role in the storage of green electricity. Regarding to the carbon emissions of green ammonia, Lee et al. reported that the well-to-plant-gate greenhouse gas (GHG) emissions of renewable ammonia was zero since it used zero carbon electricity such as solar and wind power [22]. However, other studies reported that the green ammonia has a carbon intensity of 0.09–0.70 tCO_2e/t [19,24,25]. To the best of our knowledge, techno-economic-environmental assessments of the low-pressure HB process are insufficient. Additionally, the cold energy of liquid ammonia usually was not taken into account in previous studies [26,27]. Significant latent heat of vaporization can be used in ammonia utilization, the cold energy should be considered in energy efficiency analysis. In the case of methane and coal-based ammonia production, the purge gas exhausted by the HB loop are usually combusted as fuel [28]. However, in the case of green ammonia production, the purge gas should be deeply recovered. The NH_3 emissions after the recovery of the purge gas should be assessed and controlled, as ammonia has a hazardous impact on human health and air quality.

The objective of this study is to investigate the feasibility and competitiveness of a low-pressure HB process for the production of green ammonia. A power-to-ammonia process model integrated with two designs of low-pressure HB synthesis loops was established using a common process simulator, and then multi-perspective assessments were performed, including indicators of unit power consumption, energy efficiency, LOCA, life cycle greenhouse gas, and ammonia emissions. This study provides valuable guidance for future research and helps in decision-making at different stages of this technical route.

2. System description and modeling

2.1. System description

Fig. 1 shows the system of power-to-H_2-to-NH_3 process integrated with low-pressure HB units. It comprises three units: a water electrolysis unit (WEU) for H_2 production, an air separation unit (ASU) for N_2 production, and a Haber-Bosch unit (HBU) for ammonia synthesis and separation. The following analyses of the contributions of energy consumption, equipment cost, and environmental impact are discussed based on these three units.

2.1.1. WEU for H_2 production

The purity of the H_2 feed gas from the ammonia synthesis should be at least 99.999 mol.% [3,19]. Several electrolytic technologies are available for hydrogen production from water. Alkaline electrolysis cells (AEC) and proton-exchange membrane electrolysis cells (PEMEC) are well-developed and commercially available. As the most mature technology, the equipment cost of AEC has reduced significantly in recent years in China, and most of the latest AECs operate at 1.5 MPa. An increasing number of projects employ PEMEC for green hydrogen production owing to their advantages, such as high efficiency, high-purity of produced hydrogen, quick cold start, and quick load change

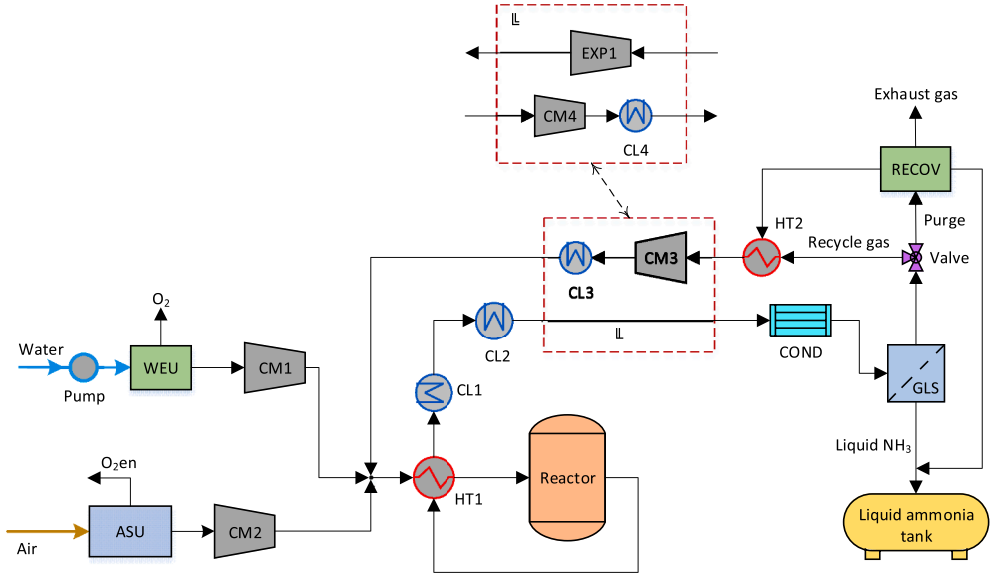

Fig. 1. Power-to-ammonia process integrated with low-pressure (LP) and ultra-low-pressure (ULP) HB synthesis techniques.

capacity. Solid oxide electrolysis cells (SOEC) can potentially offer the most efficient electrolysis process and minimize specific power consumption. However, this technology requires large-scale research and demonstration to reach the commercial stage. Table 1 lists the state-of-the-art and future (Target 2050) performance indicators for these technologies [29]. The hydrogen produced was then compressed using compressor CM1 for the following synthesis.

2.1.2. ASU for N_2 production

The purity of the N_2 feed gas from the ammonia synthesis should be at least 99.99 mol.% [19]. It is recommended to use cryogenic distillation techniques to produce N_2 with a purity greater than 99.99 % and a flow rate greater than 10,000 Nm^3/h [30,31]. Considering the scale and decentralized characteristics of renewable energy projects, as well as the current scales of ammonia production factories, this work sets 30 t/h as the baseline scale for green ammonia synthesis. The flow rate of N_2 was approximately 19,800 Nm^3/h. Therefore, to ensure the N_2 purity, the cryogenic distillation technology is employed with an operating pressure of 0.6 MPa and a specific power consumption of 0.23 kWh/kg N_2. [32] The nitrogen produced was compressed using a compressor CM2 to meet the synthesis requirements.

2.1.3. HBU for ammonia synthesis and separation

The overall reaction of the HB process is $N_2 + 3H_2 = 2NH_3$. Single-pass conversion in the HB process is typically 10–15 % [15,17], with overall conversions of 97–99 % [17]. Other studies have reported typical single-pass conversions of 20 % [26,19] and 30 % [19]. The H_2/N_2 ratio is approximately 3.0 [19], and the synthesis temperature is set to 400 °C, which are not key variables in this study. According to current Haber synthesis applications and research, the synthesis pressure is typically between 10 and 30 MPa. With technological developments, synthesis processes below 10 MPa have gradually matured. Shamiri and Aliabadi studied the modeling and analyzed an HB reactor with p_{syn} of 8.6 MPa [15]. Catalysts for ammonia synthesis were focused on recent advances at lower synthesis pressures (as low as 0.1 MPa) [33]. However, key performances such as the reaction rate and space velocity were much better when p_{syn} increased to 10 bar or higher (especially above 30 bar) [12]. Therefore, the pressures used in this study range from 10 to 150 bar. Condensation separation is the only commercially available technology for separating ammonia from synthesis products. However, this method failed when the separation pressure was below 50 bar [34]. This indicates that the condensation separation pressure is the key limiting parameter in low-pressure HB processes. Two low-pressure HB processes were designed to coordinate the pressures of the synthesis and separation steps.

1) Low-pressure HB technique (LP). When p_{syn} was greater than or equal to 8 MPa, the synthesis product was successively cooled by HT1, CL1, and CL2 to recover heat energy. The synthesized product was introduced into a condensation device (COND) at ambient temperature. Cooling energy was provided by an ammonia refrigeration system with a coefficient of performance (COP) of 2.5. The output mixture then enters a gas-liquid separator (GLS), where liquid ammonia is discharged from the bottom, and non-condensable gases (unreacted N_2, H_2, and Ar) are discharged from the top. The feed gas of the power-to-ammonia process contains fewer impurities than natural or coal-based feed gas. Most gases (99.9 %) were recycled and utilized as feedstock. A total of 0.1 % of the gases released from the separator (purge gas) were discharged into the RECOV unit. Pressure swing adsorption and cryopreservation equipment were used to recover 99 % of the H_2 and 99.9 % of the NH_3 in the purge gas, and the energy demand was estimated with a COP of 1.6 [35]. The recovered H_2 was also recycled and used as feedstock for the synthesis reaction.
2) Ultra-low-pressure HB technique (ULP). When p_{syn} was <80 bar, the synthesis product was cooled first. Subsequently, as shown in dashed box 2 in Fig. 1, the product was compressed to 80 bar or higher, and the stream was cooled to the ambient temperature. The refrigeration, condensation, and separation processes were the same as those in the conventional HB process. In this case, the pressure of the recycled gas was significantly higher than that of the feedstock from the ammonia synthesis. Therefore, the recycled gas preheated by HT2 is introduced into expander EXP1 to generate electricity by utilizing the pressure energy. This system uses electricity to offset part of the electricity consumption.

Table 1
Key performance indicators of AEC, PEMEC, and SOEC technologies for hydrogen generation.

	Scenario	SPC_{H2} (kWh/kg)	Pressure (bar)
AEC	Current	50–78	<30
	Future	<45	>70
PEMEC	Current	50–83	≤50
	Future	<45	>70
SOEC	Current	40–50	1
	Future	<40	>20

2.2. Process modeling

The process models were built using Aspen Plus 10.2. The simulation was performed based on the template of the ammonia model in Aspen Plus© with modifications as well as related modeling works [9,26,36,50]. The—Redlich–Kwon Soave–Boston Mathias (RKS-BM) method was selected because of its compatibility with gas processing and refinery applications. The process flowsheets of power-to-ammonia with the LP and ULP techniques in Aspen Plus are shown in Figures S1 and S2. Depending on the pressure ratio, a single- or multi-stage compressor was applied. The model blocks and operational parameters of the key devices are listed in Table S1. As listed in Table S2, the HB process was successfully modeled by verification based on the publications of Riotto et al. [9] and Zuo [37].

3. Assessment methodologies

3.1. Technical assessment

Ammonia with a purity of 99.5 % is typically produced at the industrial level [19]. The specific power consumption of ammonia (SPC_{NH3}) is defined as follows:

$$SPC_{NH3} = \frac{P_S}{m_{NH3}} \ (\text{kWh / kg } NH_3) \tag{1}$$

where m_{NH3} is the mass flow rate of NH_3 in t/h and P_{Sys} is the total input power of the power-to-ammonia process in MW, which is calculated as follows:

$$P_{Sys} = P_{PW} + P_{WE} + P_{ASU} + P_{CM1} + P_{CM2} + P_{HBU} \tag{2}$$

P_{PW}, P_{WE}, P_{ASU}, P_{CM1}, P_{CM2}, and P_{HBU} are the input powers of the water pump, water electrolyzer, air separation unit, compressors CM1 and CM2, and HBU, respectively, in MW. P_{HBU} is the total input power of the HBU in MJ/h. The low-pressure HB process mainly consists of the input power of the compressor CM3 (P_{CM3}) and refrigeration (P_{Refrig}). The ultralow-pressure HB process was calculated as follows:

$$P_{HBU} = P_{CM4} + P_{Refrig} - P_{EXP1} \tag{3}$$

where P_{EXP1} is the output power of the expander EXP1 in MW.

Energy efficiency is a common indicator of energy conversion and storage. To facilitate future comparative analysis, the systematic energy efficiency of the whole process (η_{PtA}) is analyzed as follows:

$$\eta_{PtA} = \frac{m_{NH3} \cdot LHV_{NH3}}{3.6P_S} \times 100\% \quad (4)$$

where LHV_{NH3} is the lower heating values of NH_3 in MJ/kg.

The energy efficiency (η_{PtA+}) including cold energy of ammonia is calculated as follows:

$$\eta_{PtA+} = \frac{m_{NH3} \cdot (LHV_{NH3} + \gamma_{NH3})}{3.6P_S} \times 100\% \quad (5)$$

where the γ_{NH3} is the cold energy of liquid ammonia, which consists of the latent heat of vaporization and sensible heat relative to 0 °C.

3.2. Economic assessment

The scale baseline is 30 t/h of ammonia. The systems and equipment were designed and sized based on the existing ammonia factories. The benchmark year was 2022. The economic evaluation aims to determine the levelized cost of ammonia (*LCOA*) as the minimum selling price of ammonia that yields a net present value (*NPV*) of zero at the end of the plant lifetime [11,38]. The *NPV* is calculated by summing the annualized cash flows.

$$NPV = \sum_{t=0}^{l} \frac{ACF_t}{(1+i)^t} \quad (6)$$

where *ACF* is the annualized cash flow, *l* is the project lifetime (25 years), *i* is the discount factor (8 %). Capital expenditures (CAPEX) include direct costs, indirect costs, contingency and fee costs, and auxiliary facilities costs, which are estimated based on the model listed in Table S3 for total capital investment (*TCI*). The *TCI* was then estimated using equipment costs (*EC*s). The *EC* of the equipment were calculated as follows:

$$EC = \left(EC_0 \times \frac{CEPCI_{2022}}{CEPCI_i}\right) \times \left(\frac{S}{S_0}\right)^n \quad (7)$$

where S_0 and EC_0 are the capacity and equipment costs of the reference case, respectively, and *S* and *EC* are the capacity and equipment costs of the planning case, respectively. *n* denotes the scale exponent [39]. *CEPCI* is a chemical engineering plant cost index that refreshes *EC* from the past to the present. Additionally, the pressure adjustment in [40] was multiplied by the costs of the reactors, heat exchangers, and compressors on a reference scale. Based on the above estimation method, Table 2 lists detailed data related to the equipment costs of the main devices of a 30 t/h power-to-ammonia plant with a synthesis pressure of 80 bar. Finally, this study assumes that 70 % of *TCI* is financed by loans with an annual interest rate of 4.9 %.

The estimated operating expenses (OPEX) are listed in Table S4. The total plant cost includes equipment costs, other direct costs (installation, building, and auxiliaries), and indirect costs (engineering and contingency). Additionally, straight-line depreciation was employed, and the salvage value was 4 %.

3.3. GHG and NH_3 emission assessment

This study focused on the life cycle greenhouse gas and ammonia emissions, as the latter can lead to tiny particles in the air that damage human health. The evaluation were performed using the life cycle assessment (LCA) framework according to the ISO standard [46]. The functional unit was 1 metric ton liquid NH_3 produced. The system boundary for this assessment is illustrated in Figure S3. Infrastructure related to the ammonia synthesis factory was not considered in this study because prior works in this area have demonstrated that the environmental impacts of infrastructure are often omitted [9,47]. The green power and natural water were considered as utilities. Then, the assessment is analyzed using SimaPro software (9.4.0.1) with the Ecoinvent 3 database and the 'Cut-off, S' method.

Table 2
Equipment costs and basis of key devices of a 30 t/h power-to-ammonia plant.

Equipment	Basis	Value	*EC* (k€)	Reference
WEU				
Water purification	Water	57.33 t/h	426	[41]
Water pump	Water	57.33 t/h	2	[41]
AEC (individual: 1000 m^3/h)	H_2	5.35 t/h	46,225	a
PEMEC (individual: 1000 m^3/h)	H_2	5.35 t/h	210,111	[42]
H_2 compressor	H_2	5.35 t/h	4186	[41]
H_2 tanks (individual: 2 MPa, 100 m^3)	H_2	21.38 t	18	[41]
ASU				
Air compressor	N_2	24.79 t/h	2962	[30]
Cooling subsystem	N_2	24.79 t/h	8374	[30]
N_2 compressor	N_2	24.79 t/h	1732	b
N_2 tanks (individual:2 MPa, 100 m^3)	N_2	99.15 t	10	[16]
HBU				
Reactors suit	NH_3	30 t/h	911	[43]
Heat exchangers suit	NH_3	30 t/h	4189	[43]
Compressor (LP)	Power	0.62 MW	84	c
Compressor (ULP)	Power	4.24 MW	385	c
Expander (ULP)	Power	3.18 MW	342	b
NH_3/CO_2 refrigerator	Power	3.08 MW	1906	[44]
NH_3 tanks	NH_3	720 t	119	d
Pressure swing adsorption	H_2 recovered	75 kmol/h	171	[45]

a: Estimated by tender price in 2023 from the centralized procurement of China Energy Engineering Group Co., Ltd.
b: Estimated by tender price in 2024 from Guoxin Suyan 2 × 250 MW compressed air energy storage project.
c: Estimated by tender price in 2022 from Hubei Yingcheng 300 MW compressed air energy storage project.
d: Estimated by quoted price in 2023 from Shandong Zhongjie Special Equipment Co., Ltd.

4. Results and discussion

4.1. Technical performances

The technical performances of both LP and ULP techniques were analyzed in this section. Unless otherwise specified, the variables were kept at their baseline values (p_{we} of 20 bar, p_{syn} of 80 bar for the LP technique, SPC_{H2} of 50 kWh/kg H_2, and single-pass conversion of 0.15).

4.1.1. Influences of p_{we} and p_{syn}

Fig. 2(a) shows the variations of η_{PtA} with p_{we} and p_{syn}. With respect to the PtA process with the LP technique, as shown on the right side of the dotted line in Fig. 2, the η_{PtA} at a given p_{we} gradually decreases with the increase in the p_{syn} from 70 bar to 150 bar. When the p_{syn} exceeds 90 bar, the decline in η_{PtA} is even smaller. A lower p_{syn} value is beneficial for reducing the power required to compress feed gas streams. Furthermore, at the same p_{syn}, the η_{PtA} rises with the increase in p_{we}, indicating that higher p_{we} is favorable to this process. Therefore, an electrolyzer that can be operated at higher pressures is preferred for the PtA process. Further analysis revealed that the average sensitivity coefficients of η_{PtA} to p_{we} and p_{syn} were 0.007 and −0.006, respectively. In general, η_{PtA} and SPC_{NH3} are not sensitive to these pressures.

The η_{PtA} with the ULP technique is at constant separation pressure of 77 bar, as shown on the left side of the dotted line in Fig. 2(a). At a given p_{we}, it generally first increased and then decreased with an increase in p_{syn} from 20 to 70 bar. The η_{PtA} achieves the highest value with p_{syn} of

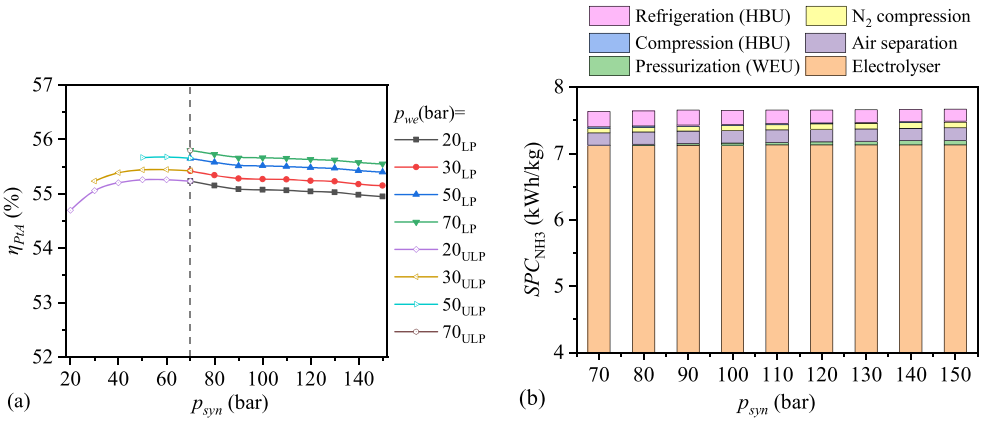

Fig. 2. Variations of (a) η_{PtA} with p_{syn} and p_{we}, and (b) contributors to SPC_{NH3}.

approximately 60 bar. This was the result of the compressors with opposite variations in power consumption. Similarly, higher p_{we} is beneficial to this process. At a given p_{we}, the optimal η_{PtA} with the ULP technique is slightly greater than that with the LP technique. For example, when p_{we} is 20 bar, the highest η_{PtA} of ULP and LP techniques are 55.26 % and 55.23 %, occurring at the separation pressures of 77 bar and 67 bar, respectively. Taking the separation pressure as the dominant constraint for the same scenario, for example, 77 bar, the highest η_{PtA} of ULP and LP techniques are 55.26 % and 55.15 %. The ULP technique has only a slight advantage in energy efficiency over the LP technique

Fig. 2(b) shows the contributors to SPC_{NH3}. To emphasize the contributions of devices in HBU, the minimum power consumption conditions are set for other units, for example, SPC_{H2} of 40 kWh/kg, p_{we} of 70 bar. Fig. 2(b) shows that the SPC_{NH3} changes very slightly with p_{syn}. The total contribution of HBU is relatively small (<3.5 %). Furthermore, the refrigeration is the main contributor to HBU's power consumption, indicating a little potential to reduce SPC_{NH3} by the optimization of HBU. The discussion on the variations of η_{PtA+} is omitted, as it is the small as that of η_{PtA}.

4.1.2. Influences of single pass conversion

As shown in Fig. 3, the η_{PtA} of the two processes gradually increases with the increase in single-pass conversion. However, the differences were minimal. η_{PtA} with the ULP technique had an average of 0.12 percentage points greater than that with the LP process. The sensitivity coefficient of η_{PtA} to single pass conversion is, on average, 0.019. This

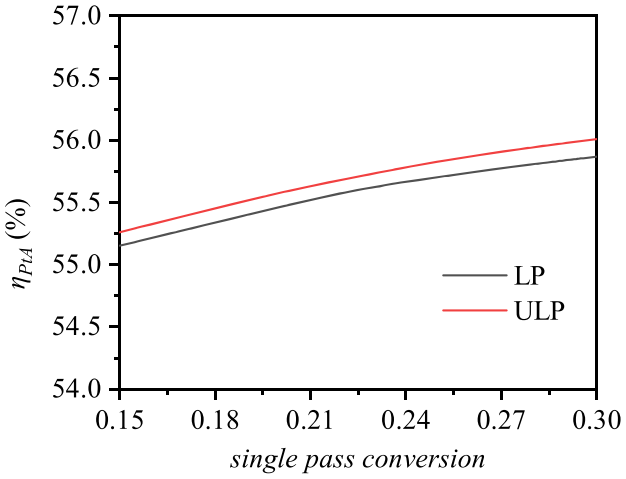

Fig. 3. Variation of η_{PtA} with single pass conversion.

implies that improving catalytic performance is potentially more efficient than optimizing pressure.

The ULP technique involves a more complex process configuration and requires an expander. Considering the current technical status, especially the flexible operation for green power utilization or storage, the ULP technique is a suitable solution for the PtA process. Therefore, it was not evaluated in the subsequent assessments. However, this technique offers a technically feasible solution for the application of an ultralow-pressure catalyst that avoids the constraints of condensation separation pressure.

4.1.3. Influences of SPC_{H2}

Fig. 4 shows that the η_{PtA} linearly decreases from 67.84 % to 46.46 % while the SPC_{NH3} linearly increases from 7.74 to 11.30 kWh/kg, with the increase in SPC_{H2} from 40 to 60 kWh/kg. The sensitivity coefficient of SPC_{NH3} to SPC_{H2} is 0.899. These results indicate that reducing SPC_{H2} is the most crucial way to improve the energy conversion performance of the PtA process integrated with the HB technique. As shown in Fig. 4(a), the η_{PtA} is lower than the corresponding energy efficiency of power to hydrogen (η_{PtH}). The SPC_{H2} of the SOEC is predicted to be below 40 kWh/kg H_2 [29]. The η_{PtH} based on higher and lower heating values related to SPC_{H2} of 39.5 kWh/kg are 99.71 % and 84.35 %, respectively. Considering that the actual process involves heat dissipation and irreversible losses, the future decline in SPC_{H2} is limited, and an SPC_{H2} of 40 kWh/kg is conservatively set as the minimum value in the future scenario.

Fig. 4(b) shows the contributions of the three units to SPC_{NH3}. In general, the electrolyzer is always the largest contributor to power consumption (>93 %), followed by refrigeration and nitrogen production, whereas the energy consumption of the remaining devices, for example compressors, accounts for very small shares (<1.5 %). As reported by Wang et al. [3], the share of hydrogen production (89.5 %) is slightly lower than that in this study, which is probably caused by the reduction in the differences in energy consumption between HBU and ASU. However, these values indicate that the electrolysis of water is the most energy-consuming step for green ammonia production, whereas the HB process takes a back seat.

4.1.4. Optimal technical indicators

The optimal technical indicators of PtA using the LP technique are listed in Table 3. The NH_3 purities in all cases were not <99.7 mol.%. Under the current scenario, the SPC_{NH3} of the process integrated with AEC, PEMEC, and SOEC reaches up to 9.49, 9.45, and 8.91, respectively, in kWh/kg. By contrast, under the future scenario, it could achieve 8.46, 8.43, and 7.64, respectively, in kWh/kg. The SOEC is the preferred electrolysis technology for ammonia production due to its energy conversion efficiency. The minimum SPC_{NH3} (7.64 kWh/kg) by this study is

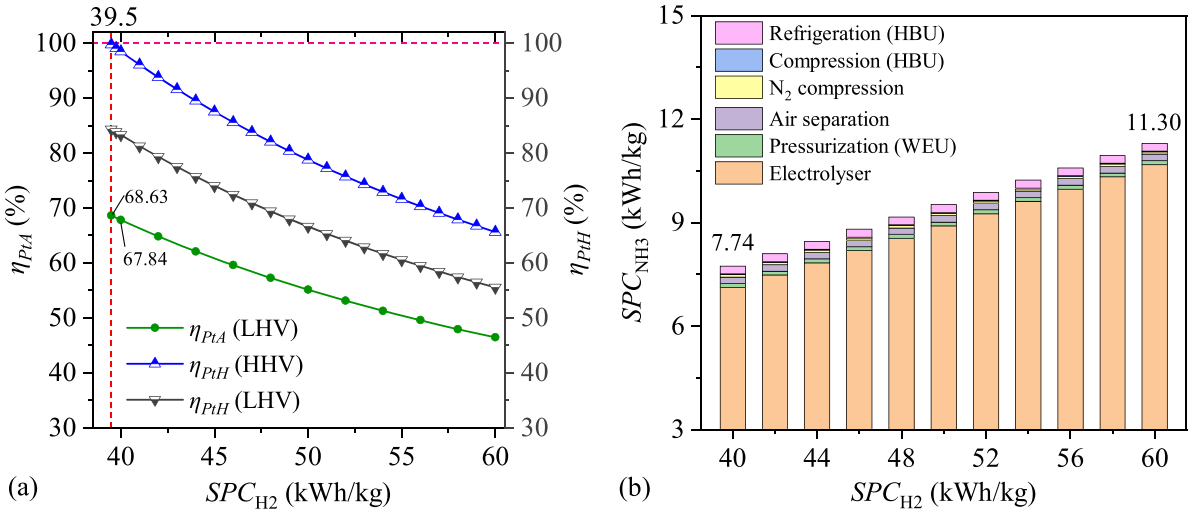

Fig. 4. Variations of (a) η_{PtA} and (b) SPC_{NH3} with SPC_{H2}.

Table 3
Optimal technical indicators of 30 tNH_3/h PtA process.

Electrolyzer	AEC		PEMEC		SOEC	
	Current	Future	Current	Future	Current	Future
p_{we}(bar)	30	50	50	70	1	20
SPC_{H2} (kWh/kg)	50	45	50	45	45	40
p_{syn}(bar)	80	70	80	70	80	70
Single-pass conversion	0.15	0.25	0.15	0.25	0.15	0.25
SPC_{NH3} (kWh/kg)	9.49	8.46	9.45	8.43	8.91	7.64
η_{PtA} (%)	55.35	62.07	55.58	62.25	58.93	68.71
η_{PtA+} (%)	59.41	66.62	59.66	66.82	63.26	73.75
Ps (MW)	285	254	283	253	267	229

comparable to that reported by Wang et al. (7.2 kWh/kg) [48]. and Qi et al. (7.4 kWh/kg) [49], which were also based on SOEC. The η_{PtA} is in the range of 55.35–58.93 % and 62.07–68.71 % under the current and future scenarios, respectively. These efficiencies can be used to estimate the energy efficiency of the power-to-ammonia-to-power or energy systems. η_{PtA+} varies from 59.41 % to 73.75 %. η_{PtA+} is 4 – 5 percentage points greater than η_{PtA}, indicating that the cold energy should be considered in energy efficiency analysis, and it should also be sufficiently used in ammonia utilization stage.

The systematic power consumption *Ps* represents the ability of a plant to utilize or store green power. For a 30 tNH_3/h plant, *Ps* varies from 229 to 285 MW, which is comparable to that of a medium-sized pumped-storage plant or a large compressed-air energy-storage plant.

4.2. Economic assessment

In this section, the economic assessment of both LP and ULP techniques was performed based on the baseline technical performance of the process integrated with AEC in the current scenario. A scale of 30 t/h, electricity price of 0.041 €/kWh, and equivalent operating hours (*EOH*) of 4000 h were also set as the baseline. Here the *EOH* means the number of hours of operation equivalent to the loading at rated capacity.

4.2.1. Configurations with LP and ULP

Fig. 5 shows that the *LCOA* with ULP technique is always greater (~1 %) than that with LP technique under the same conditions. The result is that the *ECs* of compressor and expander of ULP technique are much greater than that of LP technique (Table 2), the advantage in η_{PtA} with ULP technique is too slim (~0.12 %). Taken together, the PtA with LP technique is recommended to use for HB synthesis, and only this technique is focused on in the following assessment. However, it should be noted that the separation method in ULP technique (compression of synthesis product and expansion of recycle gas) is feasible and affordable, it can be employed for other low-pressure synthesis technologies, such as ammonia synthesis of electrocatalysis and plasma catalysis.

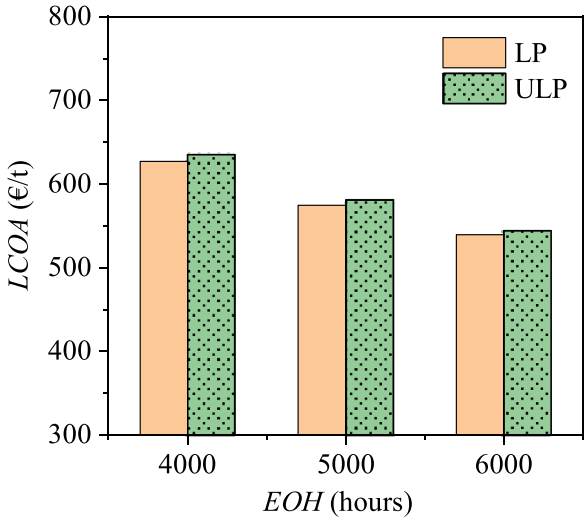

Fig. 5. *LCOA* with LP and ULP techniques.

4.2.2. Equipment cost

As shown in Fig. 6(a), the total equipment costs (EC_T) of a 30 t/h PtA plant integrated with AEC and PEMEC are 71 and 234, respectively, in million €, at the current state-of-the-art. This difference was caused by the cost of the electrolyzer. The share of the WEU equipment costs exceeded 70 %. Although the equipment costs of electrolyzers have decreased significantly recently, electrolyzers remain the most expensive equipment in the system. There is a potential for further reduction in the equipment costs of various types of electrolyzers. The number in the form of the subscript of *EC* shown in Fig. 6 denotes the percentage of the future electrolyzer equipment cost of the current AEC equipment cost. Fig. 6(a) shows that when the electrolyzer's EC (EC_{we}) is reduced to 40 % of the current AEC's EC ($EC_{40\ \%}$), the total equipment cost is 43 million €, and the share of the electrolyzer is close to 50 %.

Fig. 6(b) shows that at an electricity price of 0.041 €/kWh, the *LCOA*

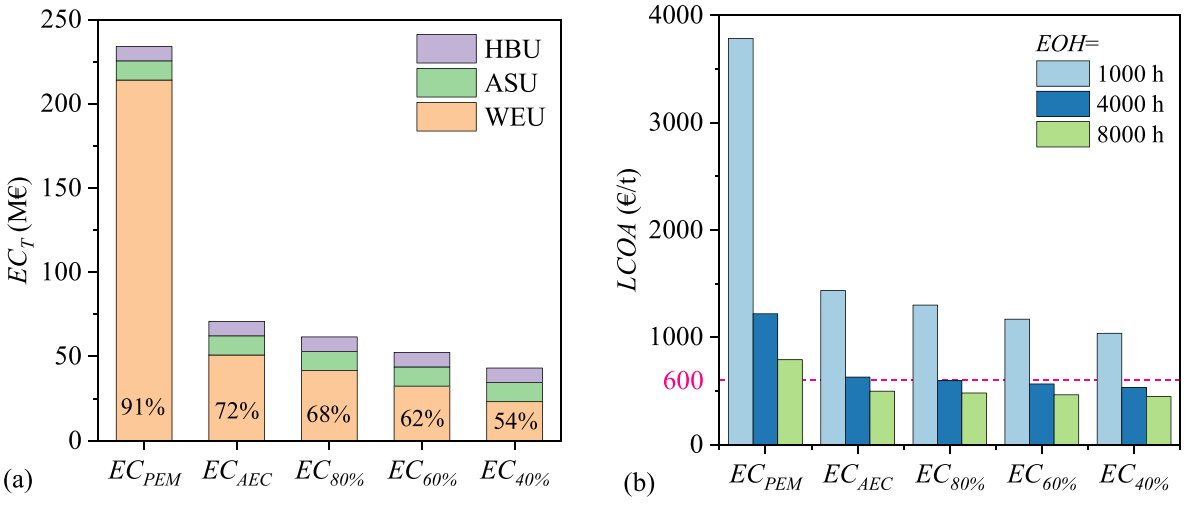

Fig. 6. Variations of (a) EC_T and (b) *LCOA* with EC_{we}.

decreases almost linearly with a decrease in EC_{we}. The recent selling price of ammonia in the Chinese market ranges from 400 €/t to 600 €/t. The current cost is approximately 4.54 times more than that of AEC. Even when the *EOH* reached 8000 h, the *LCOA* was calculated to be approximately 791 €/t. The *LCOA* with the PEMEC was not profitable in terms of the baseline electricity price. The equipment cost of the PEMEC should be less than two times the current equipment cost of AEC. This indicates that low-cost AEC technology will be used in the near future, and reducing the cost of the electrolyzer is one of the most expected improvements.

Fig. 7 shows a significant initial decrease in EC_T followed by a slight decrease as p_{syn} decreases. The total equipment cost decreased by approximately 15 % when p_{syn} decreased from 150 bar to 80 bar. However, there was only a small difference in EC_T between 80 and 70 bar. The reason is that the change in p_{syn} mainly affects the costs of devices in the HBU, and their total share is not high ($\leq$ 16 %), as the electrolyzer has the greatest share in equipment cost, and the influence of p_{syn} on EC_T is weak. The *LCOA* were 657, 638, 631, and 628 €/t at p_{syn} values of 150, 100, 80, and 70 bar, respectively. It progressively decreased as the synthesis pressure decreased; however, the differences in *LCOA* between 80 and 70 bar were very small. The sensitivity coefficient of *LCOA* to p_{syn} varies from 0.06 to 0.11, increasing with the increase in p_{syn}. The results indicate that the synthesis pressure is not the key factor affecting the EC_T and *LCOA*, especially when p_{syn} is below 100 bar. Therefore, a reduction in synthesis pressure is a beneficial measure but not an imminent contradiction for PtA plants.

4.2.3. Scale and EOH

Whether green ammonia is produced as a fertilizer or an energy carrier, a reasonable scale and *EOH* should be calculated and designed to obtain more benefits. As listed in Table 2, P_s at a plant scale of 30 t/h ranges from 229 to 285 MW, which is quite large for renewable power projects. Based on this consideration, scale and *EOH* were studied together. The annual operating hours of traditional ammonia plants generally exceed 6000 h, even up to 8000 h. Guerra et al. studied the impact of operating hours on *NPV* and concluded that at least 3700 h is needed for green ammonia plants [50]. In 2022, the *EOH* of photovoltaic power projects in China was approximately 1800–2700 h [51]. Fig. 8 shows that under the same *EOH* conditions, as the scale increases from 1 t/h to 30 t/h, *LCOA* first decreases rapidly and then decreases slightly. At the same scale, *LCOA* gradually decreases with an increase in *EOH*. Fig. 7 shows that *EOH* should not be <5000 h, and the scale should not be <10 t/h. At present, most ammonia plants produce 1000–1500 metric tons per day, and the smallest ammonia plant with a conventional design has a capacity of 250 metric tons per day. Heat transfer from

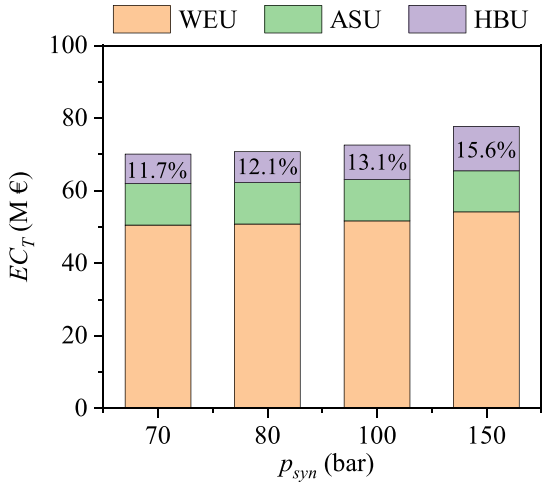

Fig. 7. Variations of EC_T with p_{syn}.

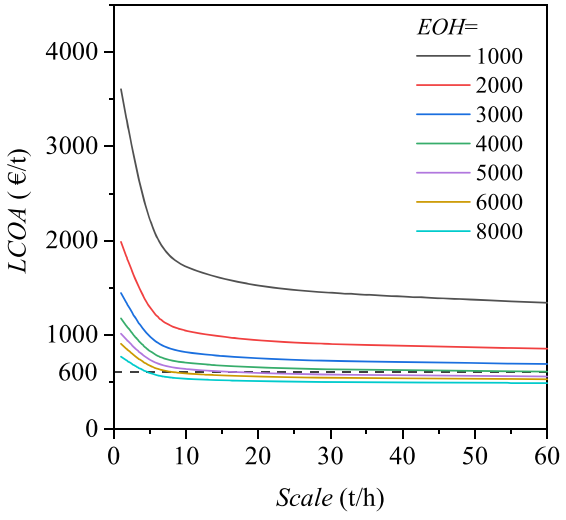

Fig. 8. Variation of *LCOA* with *scale* and *EOH*.

pipes and reactors has begun to dominate the design of ammonia plants, which produce <250 metric tons per day [19]. Our findings indicate that from the point of view of *LOCA*, the smallest plant scale is nearly the same. When a plant simultaneously meets the above requirements, changes in the *EOH* and scale do not have a significant impact on *LCOA*.

4.2.4. Electricity price and EOH

Electricity prices for energy storage may vary significantly from region to region, and even after a project is commissioned, electricity prices may be adjusted due to local policy adjustments. Therefore, the electricity price may be a long-term uncertainty factor, and its influence on *EOH* should be carefully analyzed. Liu et al. compared the life cycle cost of pumped water storage, compressed air storage, and $LiFePO_4$ battery storage extended with an electricity price (C_{El}) ranging from 0.014 to 0.057 €/kWh with a baseline value of 0.041 €/kWh [52]. With the same *EOH*, the *LCOA* increases linearly with an increase in the electricity price (0–0.057 €/kWh). At the same C_{El}, the *LCOA* decreased gradually with an increase in *EOH* (Fig. 9). The *LCOA* varies from 95 to 1591 €/t. To compete with the current ammonia market price (400–600 €/t), Fig. 9 shows that to obtain a competitive *LCOA*, the *EOH* is closely related to the electricity price, and it should be not <5000 h with the baseline electricity price.

Combined with the above figures, *EOH* is a very important factor, with a large uncertainty affecting *LCOA*. Fig. 9 also shows that the *LCOA* with electricity price of zero is still greater than 600 €/t when the *EOH* is <2000 h. Considering the general operating hours of wind and photovoltaic power projects, we believe that a green ammonia plant using PtA with the HB technique should not be purely used as an energy storage project. In this scenario, *EOH* is not sufficient. To guarantee sufficient *EOH*, the main purpose of such a plant is to produce ammonia as a chemical, and its partial capacity can be used for energy storage. This requires sufficient use of renewable power projects in a region.

4.2.5. SPC_{H2}

Fig. 10 shows an almost linear increase in *LCOA* with increasing SPC_{H2}. Although the lines in this figure appear flat because the relative change in SPC_{H2} is not large (40–50), the sensitivity coefficient of *LCOA* to SPC_{H2} is quite large, ranging from 0.51 to 0.71. Therefore, to decrease green ammonia's *LCOA*, future technological developments should prioritize the reduction of SPC_{H2}. When SPC_{H2} was <42 kWh/kg, the *EOH* was below 4000 h. In decreasing order of the absolute value of sensitivity coefficients with *EOH* of 4000 h or greater, the sequence of six variables is electricity price (0.35 – 0.78), SPC_{H2} (0.51 – 0.71), *EOH* (−0.57 – −0.27), EC_{we} (0.07 – 0.25), p_{syn} (0.06 – 0.11), and plant scale (−0.08 – −0.04). These data reveal the directions and measures for improving the profitability of green ammonia based on the low-pressure HB technique.

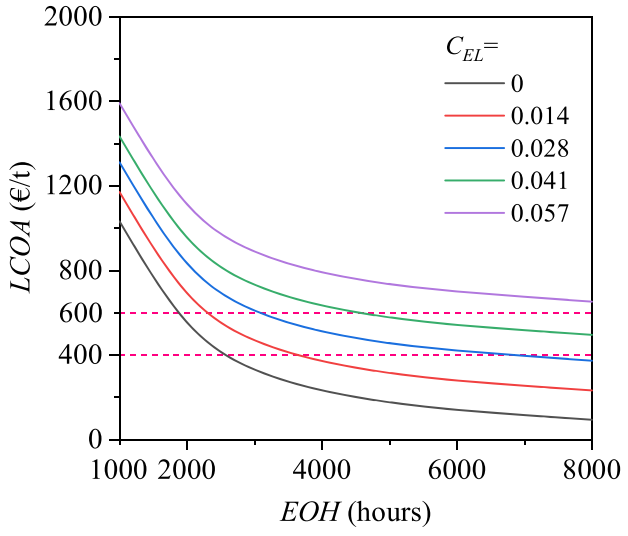

Fig. 9. Variation of *LCOA* with electricity price and *EOH*.

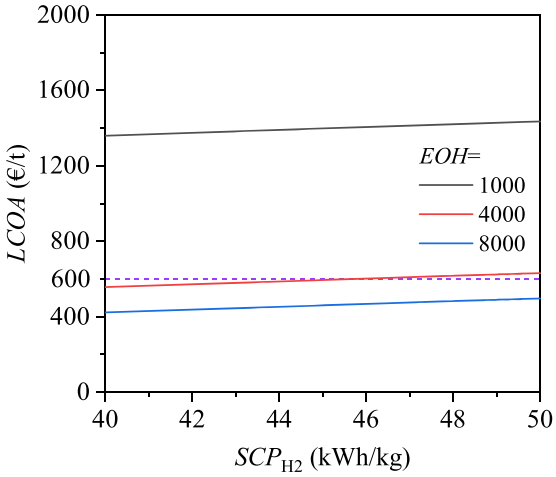

Fig. 10. Variation of *LCOA* with SPC_{H2} and *EOH*.

4.3. Life cycle GHG and NH_3 emissions

Considering the differences in configurations, efficiencies, and *LOCA*, the LP technique is focused on in the section. The life cycle GHG and NH_3 emissions were calculated based on the emission data of wind power (>3 MW) in China, and the emission factors were 0.033 $kgCO_2e$/kWh and 5.9×10^{-6} $kgNH_3$/kWh, respectively. The biogenic carbon dioxide is not considered. Based on the simulation results, the NH_3 concentration in the exhaust gas is approximately 5.8 vol.%, and approximately 0.7 kg NH_3 is exhausted when 1 metric ton of ammonia is produced.

Fig. 11(a) shows that with an increase in SPC_{H2} from 40 to 50 kWh/kg, the GHG emissions of green ammonia rise from 257 to 316 $kgCO_2e/t$, which lie within the intervals of previous data with efficient water electrolyzers (120–530 $kgCO_2e/t$) [19,20]. Furthermore, the commercial HB ammonia synthesis emits about 1.5 to 1.6 tCO_2e/t [20] and 2.41 to 4.19 tCO_2e/t [21] produced from natural gas and coal as feedstock, respectively. The green ammonia can reduce GHG emissions by 82 % and 91 %, respectively, which are comparable to the previous results [53]. Finally, the GHG emissions of ammonia produced from natural gas with CO_2 capture reduced to 0.77 $kgCO_2e/t$ [22], which is still much higher than the that of the green ammonia. Thus, green power-based ammonia is low-carbon in the life cycle perspective, and the PtA process is an effective pathway for decarbonizing the ammonia industry. Fig. 11(a) also shows that the GHG emissions from water electrolysis contribute >95 %, and the sensitivity coefficient is up to 0.94. These results imply that the GHG emissions of green ammonia can be further reduced with the progress of decarbonization in the generation of green electricity. Green power with higher carbon emissions, such as PV power, should not be used to produce ammonia.

The NH_3 emission factor of purge gas without NH_3 recovery is approximately 0.3 kg/t, and as shown in Fig. 11(b), the NH_3 emission without NH_3 recovery ranges from 0.345 to 0.356 $kgNH_3/t$. In this case, the NH_3 in the purge gas was the major contributor, with a share of >84 %. Fig. 11(c) shows that the NH_3 emission with NH_3 recovery from the purge gas reduces dramatically (0.046–0.056 $kgNH_3/t$) compared to that without NH_3 recovery. It increased slightly with an increase in SPC_{H2}. In this case, the major contributor is replaced by the water electrolysis unit (>92 %). The NH_3 emissions of liquid ammonia (Rest of World) in the Ecoinvent 3 database is approximately 0.03 $kgNH_3/t$,

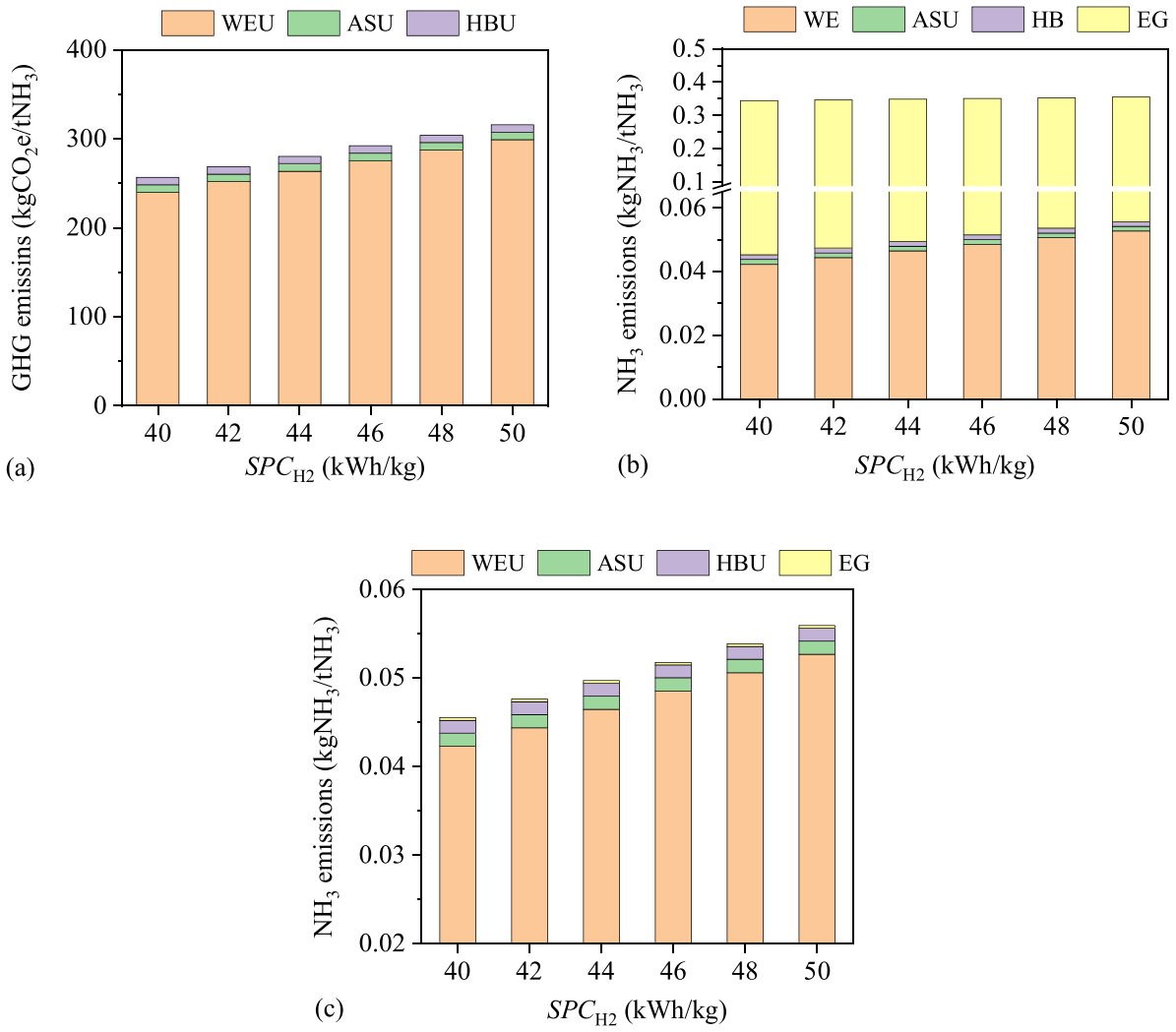

Fig. 11. Variations of (a) GHG emissions, and (b) NH_3 emission without NH_3 recovery and (c) NH_3 emission with NH_3 recovery.

which is less than the values by this study but of the same magnitude. NH_3 recovery or decomposition technologies must be employed for power-to-ammonia integration with the HB technique. The simulation results also indicated that the purge gas ratio had a significant effect on the NH_3 emissions. Additionally, based on the principle of the HB method, the development of high-performance synthetic ammonia catalysts to improve single-pass conversion can help reduce the NH_3 emissions of green ammonia.

5. Conclusion

Two PtA processes integrated with low-pressure and ultralow-pressure HB techniques were designed, simulated, evaluated, and optimized from technical, economic, and environmental aspects using energy efficiency, unit power consumption, *LCOA*, life cycle carbon, and ammonia emissions as performance indicators.

From a technical perspective, the LP technique is recommended over the ULP technique. Although the LP technique results in very slight disadvantages in energy conversion performance; however, it has a simple configuration and theoretically has higher flexibility. However, the ULP technique offers a feasible pathway for the application of low-pressure catalysts within the limitations of ammonia separation. Furthermore, the separation process in ULP technique can be used in other synthesis technologies, such as plasmas-assisted synthesis. SPC_{H2} is the key variable for improving systematic energy efficiency; in contrast, a higher electrolysis pressure, lower synthesis pressure, and higher single-pass conversion are minor measures for improving technical performance. The optimal systematic energy efficiency of the PtA process ranges from 55.35 % to 68.71 %, whereas the optimal unit power consumption of green ammonia varies from 7.64 kWh/kg to 9.49 kWh/kg, depending on different electrolyzers. The cold energy should be considered in energy efficiency analysis, and it should be sufficiently used in ammonia utilization stage.

From an economic perspective, the LP technique is recommended because the *LCOA* with LP technique is slightly lower than that with ULP technique. The decrease in synthesis pressure caused a small reduction in the total equipment cost. The plant scale should not be <10 t/h. Based on the current electricity price for energy storage in China, the *EOH* should exceed 5000 h to achieve profitability.

Regarding environmental aspects, green ammonia has very low GHG emissions (257–316 $kgCO_2e/t$) with wind power under the Chinese scenario. Green ammonia can reduce GHG emissions by >82 % compared with fossil-based ammonia. With NH_3 recovery from the purge gas, the NH_3 emissions are 0.046 to 0.056 $kgNH_3/t$, which is of the same order of magnitude as that of fossil-based ammonia.

Taken together, a green ammonia plant should not be used solely as an energy storage project but should mainly produce ammonia for chemical purposes, considering the instabilities of green power. The

deep recovery or decomposition of NH_3 in the purge gas must be employed for ammonia emission, even in the PtA process.

CRediT authorship contribution statement

Guohui Song: Writing – original draft, Methodology, Investigation, Funding acquisition, Formal analysis, Conceptualization. **Yumeng Chen:** Validation, Software, Formal analysis, Data curation. **Yingfeng He:** Writing – original draft, Software, Resources, Investigation, Formal analysis, Data curation. **Qize Jia:** Writing – original draft, Software, Investigation, Data curation. **Qingjiao Wu:** Supervision, Resources, Data curation. **Xiaobo Cui:** Validation, Software, Investigation, Data curation. **Hao Zhao:** Writing – review & editing, Supervision, Methodology, Funding acquisition, Conceptualization.

Declaration of competing interest

The authors declare that they have no known competing financial interests or personal relationships that could have appeared to influence the work reported in this paper.

Acknowledgements

This work was financially supported by the Scientific Foundation of Nanjing Institute of Technology (YKJ201818), the National Key Research and Development Program of China (2023YFE0120900), the Fund of Ministry of Education of China (No. 8091B032244), and the China National Petroleum Corporation-Peking University Strategic Cooperation Project of Fundamental Research.

Supplementary materials

Supplementary material associated with this article can be found, in the online version, at doi:10.1016/j.nexus.2025.100379.

Data availability

Data will be made available on request.

References

[1] P. Mayer, A. Ramirez, G. Pezzella, B. Winter, S.M. Sarathy, J. Gascon, et al., Blue and green ammonia production: a techno-economic and life cycle assessment perspective, iScience 26 (2023), https://doi.org/10.1016/j.isci.2023.107389.
[2] Y. Kojima, M. Yamaguchi, Ammonia as a hydrogen energy carrier, Int. J. Hydrogen. Energy 47 (2022) 22832–22839, https://doi.org/10.1016/j.ijhydene.2022.05.096.
[3] L. Wang, M. Xia, H. Wang, K. Huang, C. Qian, C.T. Maravelias, et al., Greening ammonia toward the solar ammonia refinery, Joule 2 (2018) 1055–1074, https://doi.org/10.1016/j.joule.2018.04.017.
[4] J.V. Perales-Rondon, D. Rojas, W. Gao, M. Pumera, Copper 3D-Printed electrodes for ammonia electrosynthesis via nitrate reduction, ACS Sustain. Chem. Eng. 11 (2023) 6923–6931, https://doi.org/10.1021/acssuschemeng.2c06851.
[5] X. Zhao, Q. Geng, F. Dong, K. Zhao, S. Chen, H. Yu, et al., Boosting the selectivity and efficiency of nitrate reduction to ammonia with a single-atom Cu electrocatalyst, Chem. Eng. J. 466 (2023) 143314, https://doi.org/10.1016/j.cej.2023.143314.
[6] H. Zhao, G. Song, Z. Chen, X. Yang, C. Yan, S. Abe, et al., In situ identification of NNH and N2H2 by using molecular-beam mass spectrometry in plasma-assisted catalysis for NH3 synthesis, ACS. Energy Lett. 7 (2022) 53–58, https://doi.org/10.1021/acsenergylett.1c02207.
[7] Y. Wang, W. Yang, S. Xu, S. Zhao, G. Chen, A. Weidenkaff, et al., Shielding protection by mesoporous catalysts for improving plasma-catalytic ambient ammonia synthesis, J. Am. Chem. Soc. 144 (2022) 12020–12031, https://doi.org/10.1021/jacs.2c01950.
[8] D.R. MacFarlane, P.V. Cherepanov, J. Choi, B.H.R. Suryanto, R.Y. Hodgetts, J. M. Bakker, et al., A roadmap to the ammonia economy, Joule 4 (2020) 1186–1205, https://doi.org/10.1016/j.joule.2020.04.004.
[9] T. Riotto, G. Cao, W.L. Luyben, J. Baltrusaitis, Atmospheric pressure DBD plasma ammonia synthesis and separation process design and environmental impact assessment, ACS Sustain. Chem. Eng. 9 (2021) 13233–13244, https://doi.org/10.1021/acssuschemeng.1c04031.
[10] D. Wen, M. Aziz, Techno-economic analyses of power-to-ammonia-to-power and biomass-to-ammonia-to-power pathways for carbon neutrality scenario, Appl. Energy 319 (2022) 119272, https://doi.org/10.1016/j.apenergy.2022.119272.
[11] C. Arnaiz del Pozo, S Cloete, Techno-economic assessment of blue and green ammonia as energy carriers in a low-carbon future, Energy Convers. Manage 255 (2022) 115312, https://doi.org/10.1016/j.enconman.2022.115312.
[12] K. Era, K. Sato, Miyahara S ichiro, T. Naito, K. De Silva, S. Akrami, et al., Catalytic behavior of K-doped Fe/MgO catalysts for ammonia synthesis under mild reaction conditions, ChemSusChem 16 (2023) 1–9, https://doi.org/10.1002/cssc.202300942.
[13] N. Morlanés, W. Almaksoud, R.K. Rai, S. Ould-Chikh, M.M. Ali, B. Vidjayacoumar, et al., Development of catalysts for ammonia synthesis based on metal phthalocyanine materials, Catal. Sci. Technol. 10 (2020) 844–852, https://doi.org/10.1039/c9cy02326g.
[14] Z. Li, Y. Lu, J. Li, M. Xu, Y. Qi, S.W. Park, et al., Multiple reaction pathway on alkaline earth imide supported catalysts for efficient ammonia synthesis, Nat. Commun. 14 (2023) 1–12, https://doi.org/10.1038/s41467-023-42050-7.
[15] A. Shamiri, N. Aliabadi, Modeling and performance improvement of an industrial ammonia synthesis reactor, Chem Eng J Adv 8 (2021) 100177, https://doi.org/10.1016/j.ceja.2021.100177.
[16] H.K.R. Rouwenhorst, Power-to-ammonia-to-power (P2A2P) For Local Electricity Storage in 2025 Current developments, Process Proposal & Future Research Required, University of Twente, 2018.
[17] K.H.R. Rouwenhorst, A.G.J. Van der Ham, L. Lefferts, The renaissance of the Claude process, Int. J. Hydrogen. Energy 46 (2021) 21566–21579, https://doi.org/10.1016/j.ijhydene.2021.04.014.
[18] R. Mahmud, S.M. Moni, K. High, M. Carbajales-Dale, Integration of techno-economic analysis and life cycle assessment for sustainable process design – A review, J. Clean. Prod. 317 (2021) 128247, https://doi.org/10.1016/j.jclepro.2021.128247.
[19] E.R. Morgan, J.F. Manwell, J.G. McGowan, Sustainable Ammonia Production from U.S. Offshore Wind Farms: a Techno-Economic Review, ACS Sustain. Chem. Eng. 5 (2017) 9554–9567, https://doi.org/10.1021/acssuschemeng.7b02070.
[20] O.A. Ojelade, S.F. Zaman, B.J. Ni, Green ammonia production technologies: a review of practical progress, J. Environ. Manage 342 (2023) 118348, https://doi.org/10.1016/j.jenvman.2023.118348.
[21] China City Greenhouse Gas Working Group, 2022. China products carbon footprint factors database. https://lca.cityghg.com/ (accessed April 7, 2024).
[22] K. Lee, X. Liu, P. Vyawahare, P. Sun, A. Elgowainy, M. Wang, Techno-economic performances and life cycle greenhouse gas emissions of various ammonia production pathways including conventional, carbon-capturing, nuclear-powered, and renewable production, Green. Chem. 24 (2022) 4830–4844, https://doi.org/10.1039/d2gc00843b.
[23] S. Ghavam, C.M. Taylor, P. Styring, The life cycle environmental impacts of a novel sustainable ammonia production process from food waste and brown water, J. Clean. Prod. 320 (2021) 128776, https://doi.org/10.1016/j.jclepro.2021.128776.
[24] Y. Bicer, I. Dincer, C. Zamfirescu, G. Vezina, F. Raso, Comparative life cycle assessment of various ammonia production methods, J. Clean. Prod. 135 (2016) 1379–1395, https://doi.org/10.1016/j.jclepro.2016.07.023.
[25] A. Electricity, A.J. Boero, K. Kardux, M. Kovaleva, D.A. Salas, J. Mooijer, et al., Environmental life cycle assessment ofammonia-based electricity, Energies 14 (2021) 1–20.
[26] F. Cameli, A. Kourou, V. Rosa, E. Delikonstantis, V. Galvita, K.M. Van Geem, et al., Conceptual process design and technoeconomic analysis of an e-ammonia plant: green H2 and cryogenic air separation coupled with Haber-Bosch process, Int. J. Hydrogen. Energy 49 (2024) 1416–1425, https://doi.org/10.1016/j.ijhydene.2023.10.020.
[27] H.H. Kim, Y. Teramoto, A. Ogata, H. Takagi, T. Nanba, Atmospheric-pressure nonthermal plasma synthesis of ammonia over ruthenium catalysts, Plasma Process. Polym. 14 (2017) 1–9, https://doi.org/10.1002/ppap.201600157.
[28] A.O. Oni, T. Giwa, C. Font-Palma, D.A Fadare, Comparative techno-economic and life cycle greenhouse gas assessment of ammonia production from thermal decomposition of methane and steam methane reforming technologies, Int. J. Greenh Gas Control 123 (2023) 103819, https://doi.org/10.1016/j.ijggc.2022.103819.
[29] M. Chatenet, B.G. Pollet, D.R. Dekel, F. Dionigi, J. Deseure, P. Millet, et al., Water electrolysis: from textbook knowledge to the latest scientific strategies and industrial developments, Chem. Soc. Rev. 51 (2022) 4583–4762, https://doi.org/10.1039/d0cs01079k.
[30] C. Zhu, Z. Ji, M. Huang, Comparison of several nitrogen production processes, Lowe Temp Spec Gases 41 (2023) 32–35, in Chinese.
[31] X. Lv, Comparative analysis of cryogenic nitrogen production and pressure swing adsorption nitrogen production, China Water Transp. 17 (2017) 312–314, in Chinese.
[32] O. Osman, S. Sgouridis, A. Sleptchenko, Scaling the production of renewable ammonia: a techno-economic optimization applied in regions with high insolation, J. Clean. Prod. 271 (2020) 121627, https://doi.org/10.1016/j.jclepro.2020.121627.
[33] J. Humphreys, R. Lan, S. Tao, Development and recent progress on ammonia synthesis catalysts for haber–bosch process, Adv. Energy Sustain. Res. 2 (2021) 1–23, https://doi.org/10.1002/aesr.202000043.
[34] K.H.R. Rouwenhorst, A.G.J. Van der Ham, L Lefferts, Beyond haber-bosch: the renaissance of the claude process, Int. J. Hydrogen. Energy 46 (2021) 21566–21579, https://doi.org/10.1016/j.ijhydene.2021.04.014.

[35] S. Zhang, G. Liu, Design and performance analysis of a hydrogen liquefaction process, Clean. Technol. Environ. Policy. 24 (2022) 51–65, https://doi.org/10.1007/s10098-021-02078-z.
[36] K.S. Chong, M.A. Hamid, D.K.S. Ng, Systematic decision-making framework for evaluation of process alternatives for sustainable ammonia (NH3) production, Mater. Today Proc. 64 (2022) A6–17, https://doi.org/10.1016/j.matpr.2022.07.054.
[37] Yujing Zuo, Study on Optimization Design of Synthetic Ammonia System, Beijing University of Chemical Technology, 2017.
[38] Z. Luo, C. Liu, A. Radu, D.F. de Waard, Y. Wang, J.T. Behaghel de Bueren, et al., Carbon-carbon bond cleavage for a lignin refinery, Nat. Chem. Eng. 1 (2024) 61–72, https://doi.org/10.1038/s44286-023-00006-0.
[39] C. Baumann, A. Lopatnikov, Scaling laws: uses and misuses in industrial plant and equipment replacement cost estimates, MTS J. 33 (2017) 38–44.
[40] M. Yoshida, T. Ogawa, Y. Imamura, K.N. Ishihara, Economies of scale in ammonia synthesis loops embedded with iron- and ruthenium-based catalysts, Int. J. Hydrogen. Energy 46 (2021) 28840–28854, https://doi.org/10.1016/j.ijhydene.2020.12.081.
[41] J. Xu, X. Ding, Y. Gong, G. He, T. Hu, Economic analysis of hydrogen production plant with water electrolysis, Energy Storage Sci. Technol. 11 (2022) 2374–2385, https://doi.org/10.19799/j.cnki.2095-4239.2022.0062, in Chinese.
[42] D. Song, S. Wang, J. Miao, X. Bo, Economics and cost analysis of technologies for hydrogen production from renewable energy, Sino-Global Energy 28 (2023) 24–29, in Chinese.
[43] S.A. Nosherwani, R.C. Neto, Techno-economic assessment of commercial ammonia synthesis methods in coastal areas of Germany, J. Energy Storage 34 (2021) 102201, https://doi.org/10.1016/j.est.2020.102201.
[44] X. Wu, Differentiation and Economic Analysis of R134a/CO2 Refrigeration System and NH3/CO2 Refrigeration System, J. Refrig Technol. 46 (2023) 24–27, https://doi.org/10.20094/j.issn.1674-0548.2023.04.024, in Chinese.
[45] Y. Tao, Economic analysis of different hydrogen purification technologies in coal hydrogen production, Sichuan Chem. Ind. 24 (2021) 13–16, in Chinese.
[46] ISO 14044:2006. ISO 14044:2006 Environmental management — Life cycle assessment — Requirements and guidelines. 2006.
[47] P. Arora, A.F.A. Hoadley, S.M. Mahajani, A. Ganesh, Small-scale ammonia production from biomass: a techno-enviro-economic perspective, Ind. Eng. Chem. Res. 55 (2016) 6422–6434, https://doi.org/10.1021/acs.iecr.5b04937.
[48] M. Wang, M.A. Khan, I. Mohsin, J. Wicks, A.H. Ip, K.Z. Sumon, et al., Can sustainable ammonia synthesis pathways compete with fossil-fuel based Haber-Bosch processes? Energy Environ. Sci. 14 (2021) 2535–2548, https://doi.org/10.1039/d0ee03808c.
[49] M. Qi, M. Kim, N. Dat Vo, L. Yin, Y. Liu, J. Park, et al., Proposal and surrogate-based cost-optimal design of an innovative green ammonia and electricity co-production system via liquid air energy storage, Appl. Energy 314 (2022) 118965, https://doi.org/10.1016/j.apenergy.2022.118965.
[50] C. Fúnez Guerra, L. Reyes-Bozo, E. Vyhmeister, M. Jaén Caparrós, J.L. Salazar, Clemente-Jul C. Technical-economic analysis for a green ammonia production plant in Chile and its subsequent transport to Japan, Renew. Energy 157 (2020) 404–414, https://doi.org/10.1016/j.renene.2020.05.041.
[51] National Energy Administration. National renewable energy power development monitoring and evaluation report in 2022 2022. http://zfxxgk.nea.gov.cn/2023-09/07/c_1310741874.htm.
[52] J. Wen, N. Liu, J. Pei, R. Xu, D. Liu, Life cycle cost analysis for energy storage technology, Therm. Power Gener. 50 (2021) 24–29, in Chinese.
[53] X. Liu, A. Elgowainy, M. Wang, Life cycle energy use and greenhouse gas emissions of ammonia production from renewable resources and industrial by-products, Green. Chem. 22 (2020) 5751–5761, https://doi.org/10.1039/d0gc02301a.